Revisiting pressure-induced phase transition in silicon clathrates using Ge substitution

J.-C. Blancon,[1,*] D. Machon,[1,†] V. Pischedda,[1] R. Debord,[1] P. Toulemonde,[2,3] S. Le Floch,[1] S. Pascarelli,[4] P. Mélinon,[1] and A. San-Miguel[1]

[1]*Université de Lyon, Lyon, F-69003, France; Université Claude Bernard Lyon 1, Villeurbanne, F69622, France; and CNRS, UMR5306, Institut Lumière Matière, Villeurbanne, F-69622, France*

[2]*Université Grenoble Alpes, Institut NEEL, F-38000 Grenoble, France*

[3]*CNRS, Inst NEEL, F-38000 Grenoble, France*

[4]*European Synchrotron Radiation Facility, B.P. 220, F-38043 Grenoble, France*

(Received 2 December 2015; revised manuscript received 26 February 2016; published 11 April 2016)

$Ba_8Si_{39}Ge_7$ and $Ba_8Si_{29}Ge_{17}$ have been studied at high pressure using x-ray diffraction and x-ray absorption spectroscopy (XAS) at the Ge K edge. In $Ba_8Si_{39}Ge_7$, a transition is observed similar to the one in Ba_8Si_{46}, apparently isostructural. However, the XAS data analysis shows that the transformation is related to the off-centering of the Ba atoms. A theoretical model based on a Landau potential suggests that this transition is second order, with a symmetry-breaking mechanism related to the Ba displacement probably initiated by the vacancy creation or local distortion predicted theoretically. This analysis gives a coherent picture of the phase transition mechanism. In the case of $Ba_8Si_{29}Ge_{17}$, such phase transition is not observed as the Ba atoms appear already off-center at ambient pressure.

DOI: 10.1103/PhysRevB.93.134103

I. INTRODUCTION

The first synthesis of the materials that became known as semiconductor clathrates or group-IV clathrates were reported either as a result of partial thermal decomposition of Zintl phase compounds such as NaSi or KGe [1–3] or by direct reaction between the elements [4]. There has been ongoing interest in this unusual family of solid state materials because of their unique structures and optical, electronic, and thermal properties that may have technological significance [5–7].

Several studies have addressed the high pressure behavior of type-I clathrates with filled guest cages to explore the field stability. Na_8Si_{46} apparently undergoes pressure-induced decomposition above $P = 14$ GPa, when characteristic peaks of the metallic hexagonal structure of Si begin to appear in the x-ray diffraction (XRD) pattern [5,8,9]. A different behavior is observed for larger sized guest atoms such as Ba_8Si_{46} [5,8,10–14], K_8Si_{46} [15,16], $I_8Si_{44}I_2$ [5,17], and Rb_6Si_{46} [18]. Actually, type-I clathrates with larger guest atoms exhibit an unusual volume collapse transition while apparently retaining the same cubic clathrate crystal structure followed by pressure-induced amorphization at higher pressure. This behavior and its dependence on the cage site occupancy are still not fully understood. Moreover, the apparently isostructural character of the phase transition is particularly interesting as only a few compounds exhibit such transitions.

More specifically in the case of Ba_8Si_{46}, the set of experimental results can be summarized as follows. A low-pressure transformation (3–4 GPa) has recently been proposed based on reverse Monte Carlo modeling using powder diffraction data and resistivity measurements [13]. These conclusions were used to tentatively reinterpret changes in Raman spectroscopy measurements at high pressure [14]. It is suggested that this transition is related to changes in the electronic state of Ba atoms in the large cage.

At around 7 GPa, Kume *et al.* observed a change in the Raman spectra [14]. The main change was the attenuation of a low-energy phonon mode attributed to the $Ba@Si_{24}$ coupling with the host lattice. X-ray absorption experiments, more precisely x-ray absorption near edge structure (XANES) data at the Ba L_{III} edge, indicate a change of hybridization of the Ba 5d-electrons at 5 GPa that were associated with this low-pressure transition [10]. The XRD during hydrostatic compression [He as the pressure-transmitting medium (PTM)] reveals that some thermal parameters change their behavior around 7 GPa. Below this pressure, the thermal parameters of Ba(Wyckoff site 6d), Si(24k), and Si(6c) decrease, whereas above 7 GPa, they increase [11]. Using an analysis based on the Rietveld and maximum-entropy method [12], Tse *et al.* derived the pressure-induced evolutions of the electron density distribution. They showed that Ba(6d), Si(24k), and Si(6c) atomic positions become disordered above 9 GPa. In addition, this paper concluded that a pressure-induced electronic change happens at 7 GPa; a conclusion further supported by reverse Monte Carlo calculations and resistivity measurements under pressure [13].

The most striking event at higher pressure is the presence of an apparently isostructural phase transition with a drastic change of the compressibility. The transition pressure is in the range of 13–16 GPa, depending on the hydrostatic conditions. The XANES measurements suggest a modification of the Ba-Si hybridization or the creation of a more disordered environment around Ba atoms during this transition [5]. The XRD experiments and reverse Monte Carlo modeling analysis agree on the conclusion that this transition is associated with some disordering in the Si framework [11,13]. A possible electron topological transition has been proposed as the driving force for this transformation [13]. At higher pressure, the disordering is completed as a pressure-induced amorphization occurs (at $P \approx 40$ GPa for Ba_8Si_{46}).

In summary, in the majority of silicon clathrates, the high-pressure evolution consists in minor and subtle structural

*Present address: Los Alamos National Laboratory, Physical Chemistry and Applied Spectroscopy, Los Alamos, New Mexico 87545, USA.

†Corresponding author: denis.machon@univ-lyon1.fr

modifications at low-pressure prior to an apparently isostructural phase transition followed by a pressure-induced amorphization.

To discriminate between the proposed mechanisms of these phase transitions or to provide a new explanation, information related to short-range order is required. This is the main purpose of the present paper, i.e., to obtain structural information on the Si network using x-ray absorption spectroscopy (XAS) techniques. However, the transmission of the high-pressure cell at the Si K edge ($E \sim 2$ keV) is extremely weak due to the strong absorption of the diamond anvils used to generate high pressure. To overcome this difficulty, our strategy was to work on Si/Ge-based clathrates $Ba_8(Si,Ge)_{48}$ at the Ge K-edge that is accessible even in a high-pressure configuration. We chose two different stoichiometries, $Ba_8Si_{39}Ge_7$ and $Ba_8Si_{29}Ge_{17}$, having very low and quite high degree of Ge/Si substitution, respectively. It is worth noting at this point that at low substitution degree, the presence of germanium atoms will not affect the phase transition features, as detailed below.

This paper is organized as follows. After a description of the synthesis and characterization of samples at ambient conditions, high-pressure experiments will be presented and discussed. First, we focus on XRD and extended x-ray absorption fine structure (EXAFS) results on $Ba_8Si_{39}Ge_7$. A model based on the Landau theory of phase transitions is proposed to determine the pertinent order parameter, and then the mechanism involved in the transition is discussed. Then, the experimental results on $Ba_8Si_{29}Ge_{17}$ will be shown, and the absence of volume collapse transition discussed.

II. EXPERIMENTAL

$Ba_8Si_{39}Ge_7$ and $Ba_8Si_{29}Ge_{17}$ samples were obtained by high-pressure synthesis. A stoichiometric mixture of $BaSi_2$, $BaGe_2$, Si, and Ge was treated at 3 GPa and 1073 K during an hour. The XRD patterns of the product were obtained using a Bruker D8 Advance diffractometer at the 1.54 Å wavelength. Rietveld refinements using the GSAS software [19] were performed to analyze the structure. $Ba_8Si_{39}Ge_7$ and $Ba_8Si_{29}Ge_{17}$ belong to the type-I clathrate structure, described by a space group Pm-$3n$ (No. 223) with a cell parameter $a = 10.35(1)$ Å and $a = 10.43(1)$ Å, respectively. Ge atoms are incorporated into the Si network and are all located on 24k sites, in agreement with previous results [20] (Fig. 1).

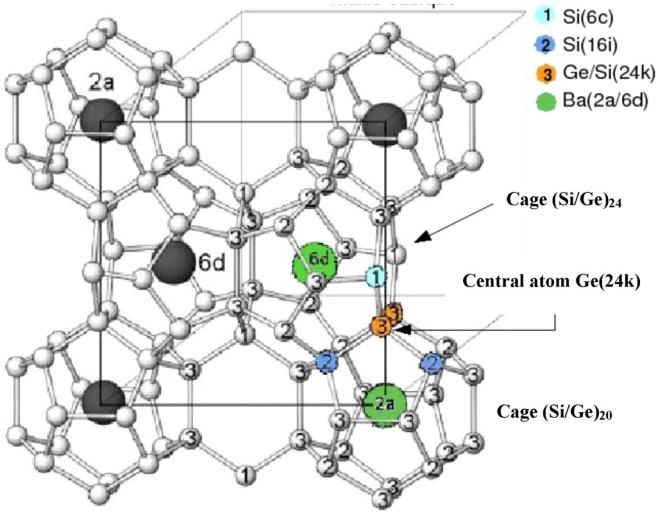

FIG. 1. Clathrate type-I structure**.** For both compositions studied here ($Ba_8Si_{39}Ge_7$ and $Ba_8Si_{29}Ge_{17}$), the Ge atoms are in 24k position. The structure is then made of mixed Si/Ge cages.

High-pressure *in situ* synchrotron experiments up to 30 GPa were carried out using a He gas membrane-driven diamond-anvil cell with diamonds having a culet size of 350 μm. In two separate experiments, $Ba_8Si_{39}Ge_7$ and $Ba_8Si_{29}Ge_{17}$ samples were loaded into a 150 μm hole drilled in a Re gasket and homogenously mixed with silicon oil, which was used as the PTM. The homogenous mixture of the sample and the PTM is essential for the quality of the x-ray absorption signal. The quantity proportion between the sample and PTM was adjusted for each sample to optimize the x-ray absorption edge amplitude and hence the signal to noise ratio of the EXAFS oscillations. The pressures were determined using the ruby fluorescence method. X-ray absorption measurements as function of pressure were carried out on the ID24 beamline at the European Synchrotron Radiation Facility [21,22]. A silicon (222) curved crystal x-ray polychromator [23] was allowed to select an energy span of ~500 eV around the Ge K-edge (11.1 keV) while focusing the beam on the sample with a full width at half maximum (FWHM) of ~20 μm. The transmitted beam was detected with a charge-coupled device (CCD) position-sensitive detector placed after the sample. The diamond anvil cell was oriented in the beam to eliminate diffraction glitches originated by the diamond single crystal diffraction.

Angular dispersive XRD patterns were also obtained at each pressure point. For this, the beam was monochromatized ($\lambda = 1.12$ Å) by placing a slit after the polychromator. Diffraction patterns were collected using image plate detection, which was inserted in the optical path between the sample and the CCD detector. The sample-to-detector distance and the image plate orientation angles were calibrated using a crystalline LaB_6 standard. The two-dimensional diffraction images were analyzed using the Fit2D software, yielding one-dimensional intensity versus diffraction angle 2θ patterns [24]. The quality of obtained XRD following the above described protocol was not enough to carry out the Rietveld refinement, and only the Le Bail refinement was performed.

The pressure evolution of the local structure of the Ge atoms was investigated by EXAFS experiments at the Ge K edge (11.1 keV). Data analysis includes the *ab initio* calculation of the atomic scattering amplitude and phase shift for each scattering path using the FEFF code [25] and the fit with the structural model using FEFFIT [26].

III. RESULTS AND DISCUSSION

A. $Ba_8Si_{39}Ge_7$

1. XRD data

Figure 2 shows the relative volume $V(P)/V_0$ as a function of pressure for $Ba_8Si_{39}Ge_7$. A change in slope is clearly observed at 14 ± 1 GPa, marking the presence of a volume collapse transition as previously observed for K-, Ba-, Rb-, and I-containing silicon clathrates (see Ref. [5] and references

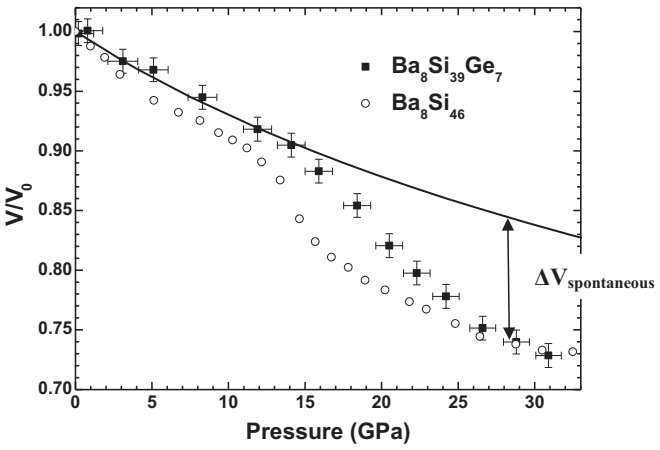

FIG. 2. V/V_0 plot for $Ba_8Si_{39}Ge_7$ as a function of pressure (points) along with a two-order Birch-Murnaghan equation of state fitted to the data with $K_0 = 119(5)$ GPa and $K_0' = 4$ (fixed) (solid line). $\Delta V_{\text{spontaneous}}$ is the difference between the calculated equation of state and the experimental data points. V/V_0 plot of Ba_8Si_{46} from Ref. [5] is also shown for comparison.

therein). There is no sign of amorphization at the highest pressure attained in the present paper, i.e., 30.8 GPa. Above the transition pressure, in the limit of our data quality, there is no obvious change in the number or relative intensities of peaks in the XRD pattern, and none of the peaks exhibit any splitting, therefore denoting the apparent isostructural character of the transition in agreement with previous results for other clathrates [5].

The $V(P)/V_0$ data obtained for Ba_8Si_{46} from Ref. [5] are also plotted in Fig. 2. The general evolution is identical, i.e., a low-pressure structure that transforms at around 14 GPa to a softer second phase. Therefore, the presence of a low amount of Ge in the host structure does not seem to affect the phase transition mechanism.

The $V(P)/V_0$ data for $Ba_8Si_{39}Ge_7$ upon compression in the pressure range 0.1–14 GPa were fitted using a second-order Birch-Murnaghan equation of state model to obtain the bulk modulus K_0 for the clathrate phase. The values obtained by this procedure were $K_0 = 119(5)$ GPa for a fixed value of $K_0' = 4$. The data quality is not sufficient to obtain reliable information by using a F-f plot as in $Rb_{6.15}Si_{46}$ [18]. However, this plot (not shown) supports the assumption of $K_0' \sim 4$. The compressibility of the $Ba_8Si_{39}Ge_7$ is therefore around 25% smaller than in its silicon counterpart [$K_0 = 93(5)$, $K_0' = 3.6$ (fixed) for Ba_8Si_{46}]. It is then important to note that the Si substitution by Ge greatly increases the mechanical properties of the clathrate. This result appears as surprising as it has been shown that in sp^3-bonded covalent systems with diamond or zinc-blend structure, the bulk modulus scales with $d^{-3.5}$, with d being the covalent interatomic distance [27]. This law applies in $Si_{1-x}Ge_x$ diamond structure alloys where the ambient pressure bulk modulus varies linearly between the two extreme compositions going from 98(Si) to 75(Ge) GPa [28]. The ambient pressure cell parameter of Ba_8Si_{46} (10.328 Å) is smaller than $Ba_8Si_{39}Ge_7$ (10.35 Å), and the same arguments would lead to a bulk modulus reduction by Ge substitution in opposition with our observations.

Several hypotheses may be invoked. First, as mentioned, in $Ba_8Si_{39}Ge_7$ the Ge substitution takes place only in the 24k sites, i.e., only in the pentagonal cycles either of the Si_{20} or the Si_{24} cages. We could then speculate that at moderate Ge substitution, the effect of Ge substitution on the electronic frustration introduced by the pentagonal cycles [29], which does not exist in the diamond structure, would have a predominant effect on the cohesive properties of clathrates. Second, bulk modulus is affected by the presence of defects. It is usual to observe only a partial filling of the cages, leading to a nonstoichiometric compound with Ba vacancies. However, calculations of bulk modulus in Ba_xSi_{46} and Rb_xSi_{46} ($x = 2$ to 8) show a variation of at most 10%. Another defect to consider is Si vacancies that have a direct impact on the network mechanical properties. For instance, in crystalline diamond silicon, the introduction of defects induces a decrease of the elastic constants [30]. It may be that syntheses of pure and mixed silicon clathrates do not generate the same amount of Si vacancies leading to a dispersion of the bulk modulus values.

For the high-pressure phase, depending on the analysis (Murnaghan equation of state or F-f plot), K_0 lies between 64 and 71 GPa with a value of K' significantly different from 4.0, indicating an important softening of the high-pressure structure. The reduced hydrostaticity of the PTM certainly affects the absolute values of the bulk modulus in that pressure domain, not enough, however, to explain the reduction by a factor of almost two, which should be then considered as a reliable result.

2. *EXAFS data*

Rietveld refinement of XRD patterns at ambient conditions, in the space group Pm-3n, indicates that the germanium atoms are positioned preferably on the 24k sites. Therefore, a given germanium atom is included into a tetrahedron, and its first neighbors are (i) a Si atom in a 6c position, (ii) two Si atoms on the 16i sites, and (iii) either a Si or a Ge atom on the 24k sites (Fig. 1). The three Si atoms in 6c and 16i can be considered as equidistant from the Ge central atom. This defines a first diffusion path. The neighboring atom on the 24k position, which is either a Si or Ge atom, defines a second diffusion path. The next main contributions in the EXAFS signal come from the Ba atoms in the cages. Two diffusion paths are then defined: one between Ge(24k) and Ba(6d) and the other one between Ge(24k) and Ba(2a). However, to minimize the number of fitted parameters both Ge-Ba paths are set as interdependent, i.e., related by a scaling factor. The main implication of this methodology is that any independent shift of Ba atoms in the sites 2a or 6d will be inaccessible. The EXAFS signal at each pressure was fitted using two parameters: the variation of the interatomic distances and the mean square relative displacement (MSRD) factor for each defined diffusion path. A selection of x-ray absorption spectra (EXAFS signal) is shown along with the corresponding fits at different pressures in Fig. 3.

From this analysis, the structural information was extracted (Fig. 4). All the path lengths (between Si/Ge and Ge and between Ba and Ge atoms) are reduced in agreement with the cell contraction obtained by XRD up to the transition pressure ($\sim$14 GPa). Above this pressure, we observe a deviation of the

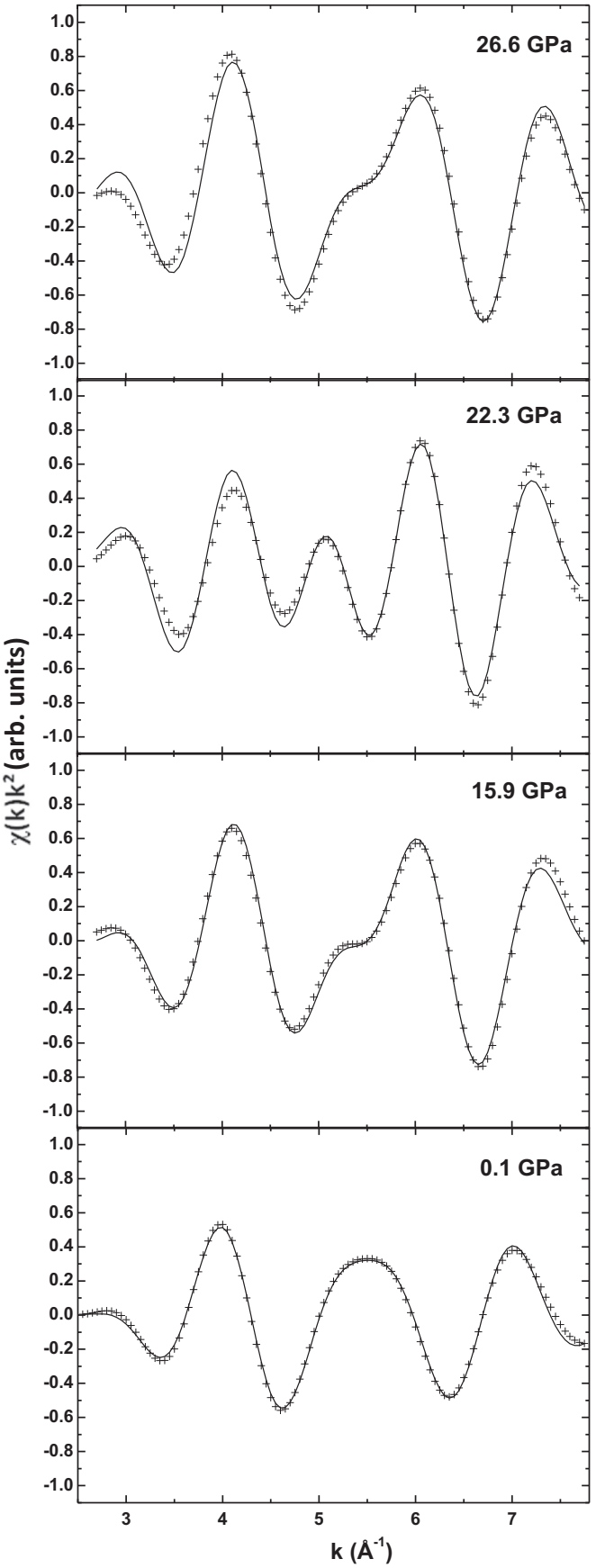

FIG. 3. Extracted EXAFS oscillations at the Ge *K*-edge together with the obtained fit at different pressures for $Ba_8Si_{39}Ge_7$.

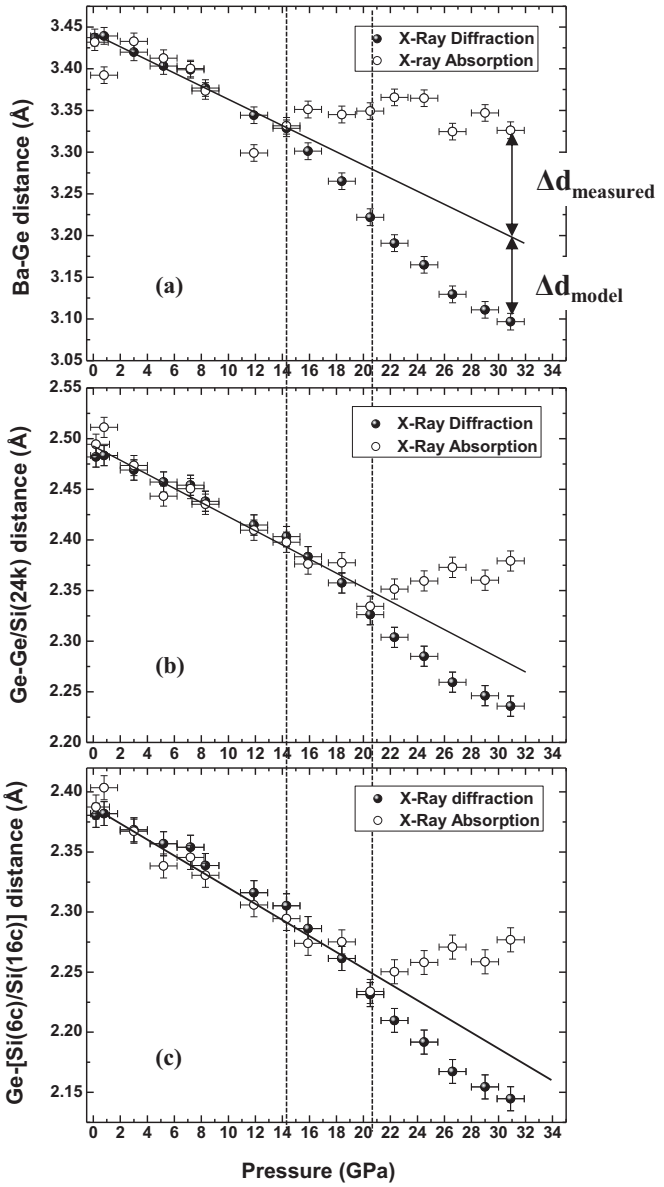

FIG. 4. Atomic distances (as a function of pressure) extracted from EXAFS analysis compared with the same parameters extracted from Rietveld refinements (XRD) and considering a totally isostructural compression. (a) Ba-Ge distance. Δd_{model} is the spontaneous distance variation linked to the volume collapse transition and calculated in a strict isostructural assumption; $\Delta d_{\text{measured}}$ is the spontaneous distance variation extracted from EXAFS data. (b) Ge-Ge(24*k*) or Ge-Si(24*k*) distance. (c) Ge-Si(16*i*) or Ge-Si(6*c*) distances

distance measured by EXAFS with respect to the one obtained by XRD. In the analysis of the XRD data, we kept the position of the atoms fixed, and we deduced the distance contraction according to an assumed homothetic volume contraction. Above ∼14 GPa, results show that the Ba-Ge distance obtained by EXAFS does not follow the homothetic transformation [Fig. 4(a)] but, surprisingly, remains almost constant up to the highest pressure reached in the experiment, i.e., 30.8 GPa. Between 14 and 20 GPa, the intratetrahedral bond lengths (Ge-Si and Ge-Ge) contraction remains homothetic [Figs. 4(b)

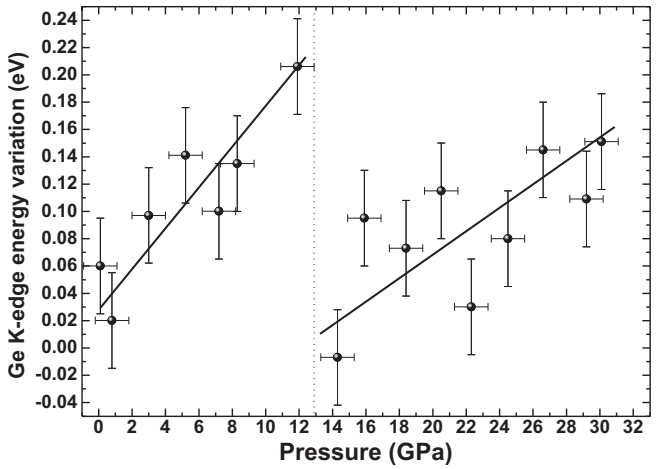

FIG. 5. Pressure-induced variation of the Ge K-edge x-ray absorption near-edge position in $Ba_8Si_{39}Ge_7$.

and 4(c)]. Therefore, one can suppose that the plateau in the evolution of the Ba-Ge length is mainly due to a shift of the Ba atom out of the cage center and away from the Ge atoms, leading to a shortening of Ba-Si distances. Such effect has already been reported from Rietveld refinement on the Ba_8Si_{46} sample where bond length shortening was observed for the majority of the Ba-Si distances [12]. This deviation in the bond length contraction is associated with a change in the energy onset of the Ge K-edge with pressure showing a sudden decrease around 12–14 GPa (Fig. 5). In addition, the MSRD factor associated to the Ge-Ba path decreases at $P \sim 14$ GPa, whereas the ones for Ge-Si or Ge-Ge paths do not show any visible deviation (Fig. 6). These features suggest a change in the electronic structure and in the coupling between Ba and Ge atoms concomitant with the displacement of the Ba atoms.

At higher pressure (starting at $P \sim 20$ GPa), a deviation from the homothetic contraction is observed for all the Ge-Si distances [Figs. 4(b) and 4(c)]. Such an effect suggests that the bond contraction reaches a limit and that the tetrahedra

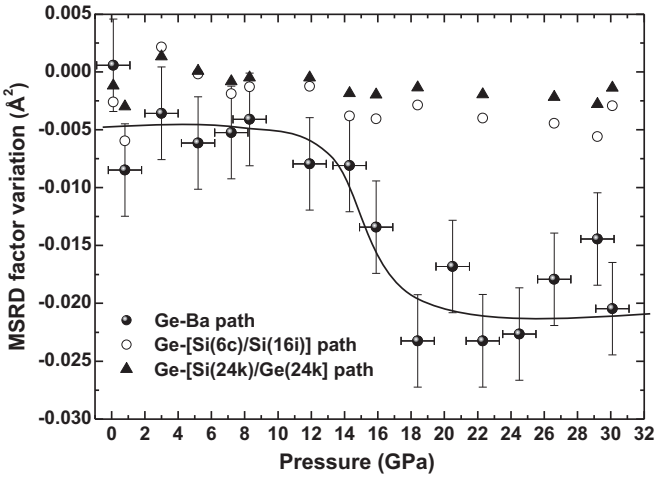

FIG. 6. Variation of MSRD factors extracted from EXAFS signal for the different paths. The errors bars are shown only for the Ge-Ba path but are similar for all paths.

undergo some distortion (torsion or flattening) to adapt to the compression. The existence of a critical distance to explain the variation of the transition pressures in the case of isostructural transformation of pure silicon clathrates has already been mentioned by San Miguel *et al.* [9].

3. Phase transition mechanism

According to the XRD data obtained on $Ba_8Si_{39}Ge_7$, the volume collapse of the clathrate structure starts at ∼14 GPa. Let us now discuss the correlations between this sudden decrease of the cell volume with the pressure-induced changes at the atomic scale. Up to 14–15 GPa, the pressure-induced variation of the interatomic distances deduced by XAS is in good agreement with the homothetic reduction of the cell volume deduced by XRD. Neither hybridization nor any displacement of the barium atoms is observed up to this pressure.

At pressures ∼14 GPa, corresponding to the volume collapse transition pressure, the barium atoms show a displacement towards Si atoms and come closer to the cages. The Ba MSRD factor obtained with the EXAFS analysis shows a sudden decrease. These conclusions are apparently in contradiction with the Rietveld analysis on XRD data that usually show an increase of the Debye-Waller parameter for Ba atoms in Ba_8Si_{46} [11] or $Ba_{24}Si_{100}$, a type-III clathrate that also shows a pressure-induced volume collapse [31]. This seeming paradox can be understood by the following considerations.

(1) The Ba displacement is incoherent, meaning that the direction of displacement is independent in each cage. The potential felt by the Ba atoms is quasispherical as the Si_{20} and Si_{24} cages are nearly regular polyhedra. The isotropic potential is confirmed by the fact that the Ba atoms sit at the center of the cages. Pressure application leads to a Ba-Si coupling and results in a Ba displacement towards Si atoms. This local symmetry breaking is statically distributed over the different Si positions. At the mesoscale, this displacement is averaged and then appears as isotropic when considering several cages.

(2) In the XRD data analysis, the Ba displacements are not included in the structural refinement as the transition is apparently isostructural. The Ba positions are considered fixed. The Debye-Waller factor, which is a free parameter, represents this incoherent displacement.

A similar situation is also met in type-II clathrate where XRD indicates that the Na atoms sit at the center of the cages whereas EXAFS data contradicts this central position [32]. Therefore, from the local point of view (at the scale of the unit cell), the pressure-induced transition is not isostructural as the Ba displacement breaks the symmetry. The coincidence between the volume variation at ∼14 GPa and the off-centering of the Ba atoms would indicate that the microscopic mechanism associated with the so-called volume collapse transition is the Ba displacement. We propose an analysis based on the Landau theory of phase transitions to check this assumption.

The choice of the Landau potential is delicate. First, it has been proposed that the transition is isostructural and of second-order type [5]. These two features are incompatible as an isostructural phase transition cannot be second order. Second, the isostructural character is strongly questioned by the present results obtained by EXAFS experiments. The

symmetry-breaking mechanism due to the Ba displacement in a given cell is averaged on several cells as totally symmetric.

In a first approach, we will treat the transition as *apparently* isostructural, and we will discuss this approximation in a second step. Isostructural transition can be described in terms of the Landau theory of phase transitions. In this case, it has been shown that the potential is [33]

$$F = F_0 + \frac{\alpha}{2}\eta^2 + \frac{B}{3}\eta^3 + \frac{\beta}{4}\eta^4, \quad (1)$$

where η is the order parameter associated to the transition. When there is no breaking of the symmetry through the phase transition, η should transform as the totally symmetric irreducible representation of the group. The physical quantity $\Delta V/V_0$ appears as a good candidate for a macroscopic order parameter, as it quantitatively changes through the transition and it is compatible with the symmetry requirement. This is similar to the density used as the order parameter for the liquid-vapor transition, a very well-known isostructural transition.

Minimization of F leads to two solutions:

(1) $\eta = 0$, which corresponds to the low-pressure phase (named hereafter phase I);

(2) $\eta = \frac{-B+(B^2-4\alpha\beta)^{1/2}}{2\beta}$, which corresponds to the high-pressure phase (phase II).

The usual conditions on the different coefficients are $B < 0$ and $\beta > 0$ [33]. The requirement on α is that it changes sign at the transition and the usual simple expression $\alpha = \alpha_0(P - P_c)$ is used, where P_C is the pressure at which phase I becomes unstable [34].

By definition, $\eta = 0$ in phase I, and one should extract the physical quantity associated to the transition. Therefore, taking $\Delta V/V_0$ as the order parameter, one should subtract the evolution related to the simple compression mechanism unrelated to the phase transition. This treatment gives access to the *spontaneous deformation* that appears at the transition and that is associated with the volume change. In Fig. 7, we show the pressure-induced evolution of the order parameter, i.e., $\Delta V_{\text{spontaneous}} = (\Delta V/V_0)$ associated to the transition and obtained by subtracting the value of $\Delta V/V_0$ calculated by the equation of state to the $V(P)$ curve (Fig. 2). The evolution of this quantity under pressure fits well with the form of the expression predicted by the theory [a change of $(\Delta V/V_0)_{\text{trans}}$ as a square root of the pressure [34]] (Fig. 7).

It has to be noted that the jump of the order parameter expected for a first-order phase transition is hardly detectable in practice, meaning that B is almost null in the Landau potential. This leads to the following approximation for Eq. (1),

$$F \approx F_0 + \frac{\alpha}{2}\eta^2 + \frac{\beta}{4}\eta^4,$$

which is the typical potential for a second-order phase transition. As a consequence, some authors have described this isostructural phase transition as being second order and associated with a displacive character. In this latter case, the expression of the order parameter in phase II is $\eta = (\frac{-\alpha}{\beta})^{1/2}$. Therefore, to model the order parameter behavior, the assumption on the order of the phase transition does not change the square root dependency with pressure. Pushing the analysis further, it is strongly suggested that the transition is not isostructural, at least in Ge-substituted clathrates. Therefore, XRD experiments on pure silicon single crystals are now required to determine the potentially new symmetry of the high-pressure phase.

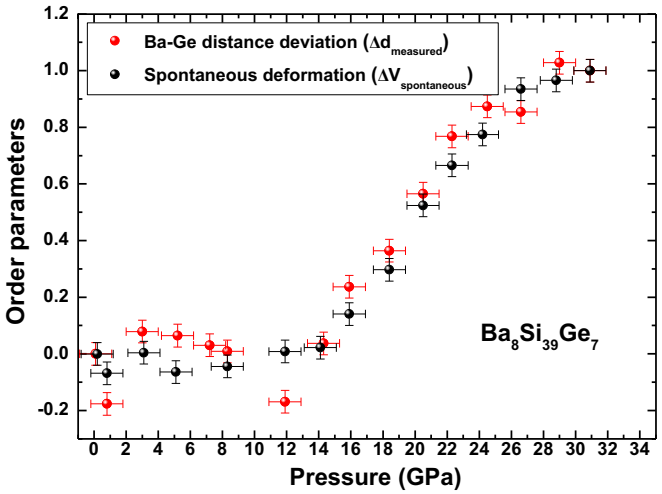

FIG. 7. Extracted order parameters: The macroscopic order parameter corresponds to the normalized spontaneous deformation ($\Delta V_{\text{spontaneous}}$; see Fig. 2), and the microscopic order parameters corresponds to the normalized deviation of the Ba-Ge distance reduction from linearity [$\Delta d_{\text{measured}}$; see Fig. 4(a)].

Despite this symmetry-breaking mechanism, $\Delta V_{\text{spontaneous}}$ remains apt to characterize the phase transition as a macroscopic order parameter.

The second step consists in relating this macroscopic quantity to a microscopic physical quantity that would describe the mechanism responsible for the phase transition. From the analysis of $Ba_8Si_{39}Ge_7$, one may reasonably assume that the off-center displacement of the Ba atoms is directly linked to the apparently isostructural transition. The process is similar to the one detailed above. From the data shown in Fig. 4(a), we extracted a spontaneous displacement of the Ba atoms [$\Delta d_{\text{measured}}$ in Fig. 4(a)] by subtracting the pressure-induced contraction of the Ba-Ge distance (fitted using a linear relation) to the Ba-Ge distance variation obtained from the EXAFS analysis.

The two *a priori* normalized order parameters (macroscopic: $\Delta V_{\text{spontaneous}}$; microscopic: $\Delta d_{\text{measured}}$) are plotted together in Fig. 7. They have the same behavior, following a square root law predicted by the theoretical analysis.

The phase transition is then characterized by a spontaneous deformation that can be related, at the microscopic level, to a displacement of the Ba atoms out of the cage centers. Such a mechanism has already been proposed using *ab initio* calculations [15] and is supported by experimental results [14]. Our analysis does not allow us to determine whether only one or both Ba atoms ($2a$ and $6d$) are implied in this transition.

The next question addresses the reason for this displacement. It could be related to a change of the potential where a

second minimum appears. This could result from a change in the hybridization between Ba and Si atoms, as suggested by previous EXAFS data at the Ba L_{III} edge. A second scenario is related to the vacancy creation, as suggested by numerical simulations [35]. This latter paper indicates that above a pressure onset, in agreement with the experimental data ($P =$ 15 GPa), Ba_8Si_{46-n} (where typically $n \approx 3$) becomes more stable than Ba_8Si_{46}. Creating n vacancies in the Si framework would lead to a softer material, as observed experimentally. In addition, the disorder generated would explain the broadening of the Raman spectra [14]. Finally, the anomalies observed at the Ba L_{III}-edge could be explained by an electronic reorganization due to the creation of dangling bonds associated with vacancies.

The stabilization of a defective structure is then consistent with our model, and vacancy creation or a rehybridization in the nanocages leading to a distortion may be the driving force of the transition. Any of those phenomena would result in a symmetry breaking mechanism leading to the Ba displacement. The statistical distribution of the vacancies or cage distortions would result in an incoherent Ba displacement. This interpretation is strengthened by our observations on $Ba_8Si_{29}Ge_{17}$, which contains more germanium atoms in substitution, as it will be detailed in the following section.

B. $Ba_8Si_{29}Ge_{17}$

1. XRD data

Figure 8 shows a plot of $V(P)/V_0$ as a function of pressure for $Ba_8Si_{29}Ge_{17}$. Contrary to $Ba_8Si_{39}Ge_7$, no apparent volume collapse transition can be observed, at least to a pressure of 36 GPa. Within the error bars, no evident structural change can be detected. This situation is similar to the germanium clathrate Ba_8Ge_{43}, which does not exhibit a pressure-induced collapse [36].

The analysis of the $V(P)/V_0$ data using the second-order Birch-Murnaghan equation of state model leads to $K_0 =$ 75(5) GPa. This value is much lower than the one obtained

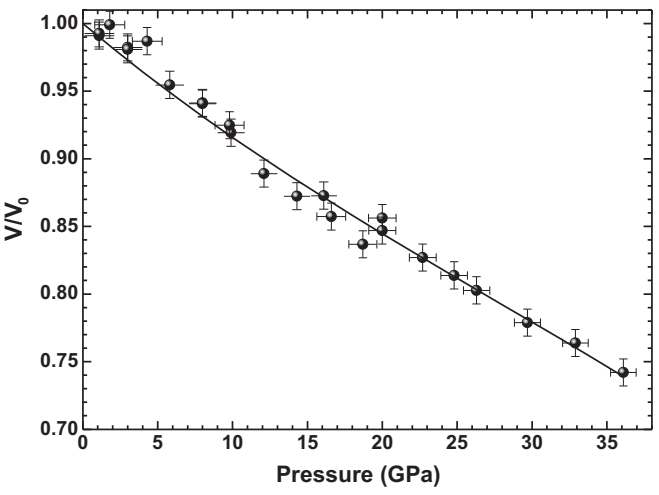

FIG. 8. V/V_0 plot for $Ba_8Si_{39}Ge_{17}$ as a function of pressure (points) along with a third-order Birch-Murnaghan equation of state fitted to the data with $K_0 = 107$ (5) GPa and $K_0{}' = 1.7(2)$ (solid line).

for $Ba_8Si_{39}Ge_7$ and for pure silicon clathrates. However, the agreement with the experimental data is poor, especially in the low-pressure range, and an F-f plot (not shown) suggests that $K_0{}'$ would be lower than 4. Using a third-order Birch-Murnaghan equation of state, we found $K_0 = 107(5)$ GPa and $K_0{}' = 1.7(2)$. Even though the value is difficult to extract, it is clear that the compression behavior is different from $Ba_8Si_{39}Ge_7$, for which $K_0{}' = 4.0$ and $K_0 = 119(5)$ GPa.

2. EXAFS data

The EXAFS data were analyzed in a first step considering only the first coordination shell, i.e., the atoms belonging to the tetrahedra described on Fig. 1. This step allows us to conclude that the germanium atoms are grouped by pairs on the 24k sites. The configuration with a silicon atom adjacent to a germanium atom is not favored for this composition, in agreement with our XRD Rietveld analysis and in agreement with the literature [20].

The model used to fit the EXAFS data takes into account the first and the second coordination shells around the germanium atoms. The structural parameters are identical to the ones of $Ba_8Si_{39}Ge_7$ except that no Ge(24k)-Si(24k) configuration has been considered as Ge(24k)-Ge(24k) is favored.

A selection of EXAFS signals with increasing pressure is shown in Fig. 9 along with the adjustment obtained using our model. The pressure evolution of the different fitted parameters is shown in Fig. 10. Since the first steps up in pressure, one can notice that the Ba-Ge distance does not change in a homothetic fashion [Fig. 10(a)]. Even though this behavior can be interpreted as off-centering displacement of the Ba atoms, no apparent volume change can be observed. A hypothesis to explain these observations is that the introduction of Ge atoms above a critical concentration modifies the potential experienced by the Ba atoms and breaks the pseudospherical symmetry, leading to a small off centering of Ba atoms even at ambient pressure. Such spontaneous off centering of guest atoms is regularly observed in ternary type-I clathrates [37]. This effect is then enhanced with pressure, leading to a larger shift of the Ba atoms. The possibility of an initial off centering of the Ba atoms may be investigated by different techniques [37], and notably it will be tested by nuclear magnetic resonance (NMR) [38] when a sufficient sample quantity will be available. In addition, the absence of pressure-induced volume collapse in Ba_8Ge_{43} [36] raises the question about a possible off centering in the pure germanium clathrate.

From ambient pressure to ∼9−10 GPa, the variation of the interatomic distances in the tetrahedra (obtained by EXAFS) evolves in agreement with the cell parameter reduction (obtained by XRD) [Figs. 10(b) and 10(c)]. At about 10–12 GPa, the Ge-Ge distance variation deviates from the homothetic model and shows a plateau until 19–20 GPa, where it starts to decrease again [Fig. 10(b)]. At pressure $P \sim 10-12$ GPa, the Ge-Si distance stops decreasing and saturates at a value slightly below 2.30 Å [Fig. 10(c)].

As in the case of $Ba_8Si_{39}Ge_7$, there exists a geometrical limit to compression after which tetrahedra start to distort. This distortion may be the driving force of the pressure-induced amorphization usually observed at higher pressure when the mechanical spinodal limit is reached [39]. In the case of

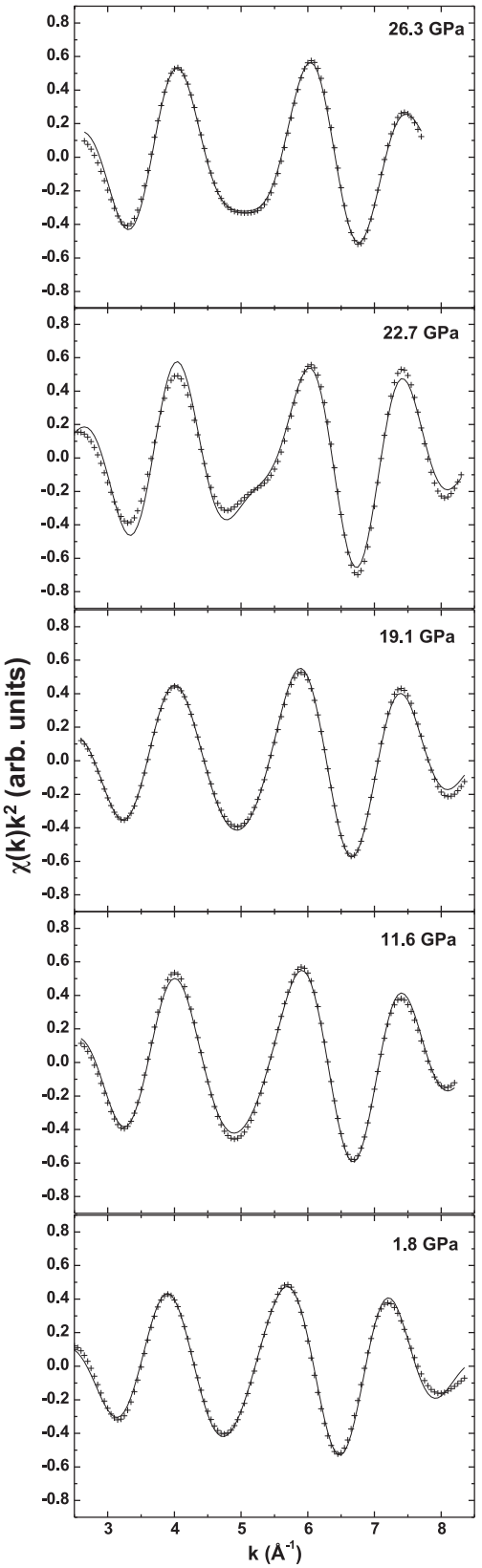

FIG. 9. The EXAFS at the Ge K-edge at different pressures for $Ba_8Si_{29}Ge_{17}$.

$Ba_8Si_{39}Ge_7$, the distortion starts when the Ge-Si and Ge-Ge distances reach ∼2.22 Å and ∼2.32 Å, respectively (Fig. 4).

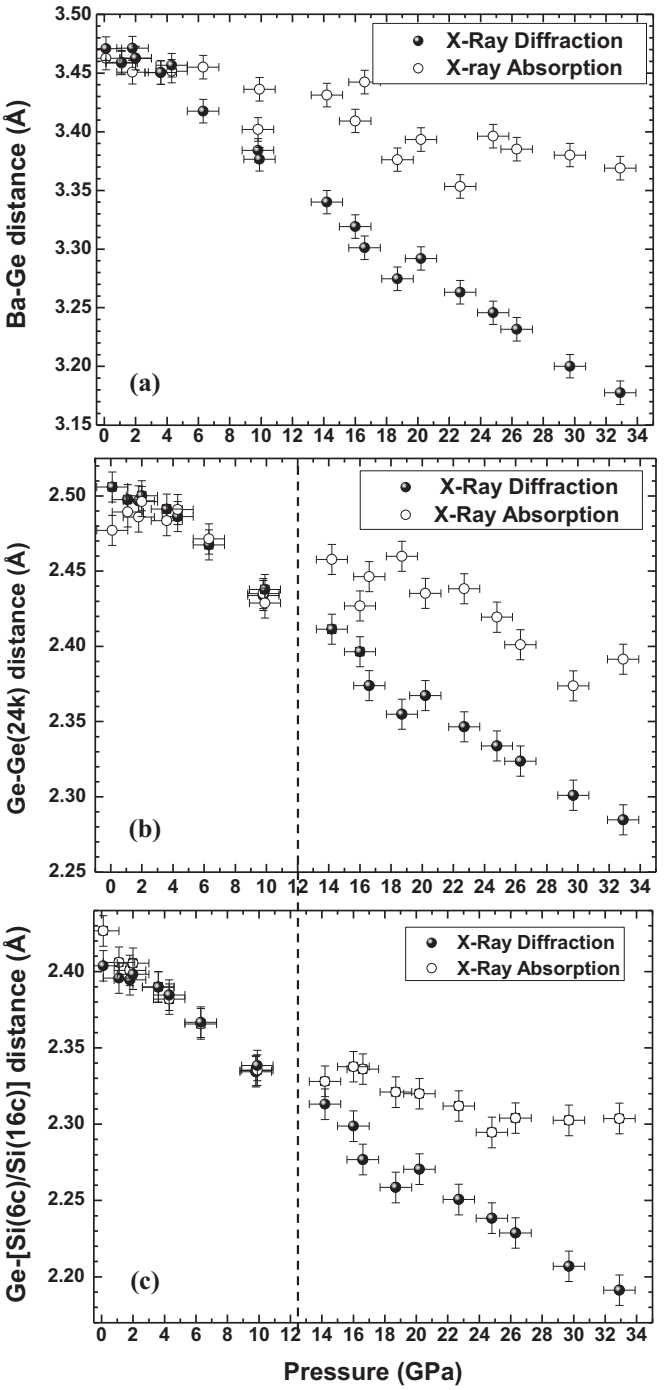

FIG. 10. Atomic distances (as a function of pressure) extracted from EXAFS analysis compared with the same parameters extracted from the cell parameters (XRD) and considering a totally isostructural compression. (a) Ba-Ge distance; (b) Ge-Ge(24k) distance; (c) Ge-Si(16i) or Ge-Si(6c) distances.

In $Ba_8Si_{29}Ge_{17}$, the distortion onset is at longer distance. The distortion starts when the Ge-Si distance is ∼2.33 Å and saturates at ∼2.30 Å (Fig. 10). For the Ge-Ge distance, the distortion occurs when the distance reaches ∼2.45 Å, it is stable during further compression until the transition, and then it decreases and reaches ∼2.37 Å at the highest pressure obtained in this paper.

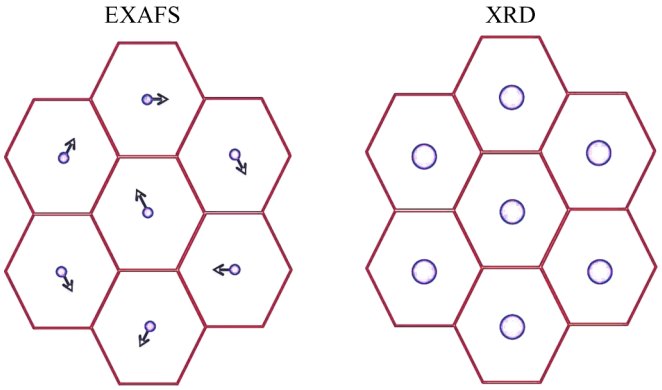

FIG. 11. EXAFS is a local probe. The data analysis shows a displacement of the Ba atoms out of the center of the cages associated with a decrease of the Debye-Waller factor. The XRD is an extended probe and gives access to an averaged structure. The increase of the Debye-Waller factor is related to the incoherent delocalization of the Ba atoms from the cage centers.

IV. CONCLUSION

The so-called volume collapse transition has been observed in many different silicon clathrate compounds. In the present paper, thanks to the incorporation of a small quantity of germanium atoms on the silicon network and by means of x-ray absorption experiments at high pressure, we were able to deepen our understanding of the local environmental evolution leading to the pressure-induced phase transition.

The analysis of the XRD patterns and of the x-ray absorption spectra at the Ge K-edge of $Ba_8Si_{39}Ge_7$ show that the transition observed at high pressure is initiated by the displacement of guest barium atoms. The driving force of the transition is discussed. The appearance of vacancies or local distortions stabilized under pressure would break the quasispherical symmetry around the Ba atoms leading to their displacements. The random distribution of such local defects would explain the isotropic displacement and the preservation of an apparently cubic symmetry at the length scale probed by XRD, a technique that relies on long-range structural coherence. With XRD, only the average structure is observed with a Ba atom apparently sitting in the center of the cages but with a more delocalized position indicated by the increase of the Debye-Waller factor, as usually observed in Rietveld refinements of XRD data [11]. Such a situation can be understood on a simplified scheme, shown in Fig. 11. This suggests that complementary techniques are required to understand phase transition mechanisms. For instance, Fourier maps differences from high quality data collected in the collapsed phase (probably better by neutron diffraction) might reveal off centering. Determining the off or on centering is clearly a major issue in type-I clathrates even at ambient pressure, and many contradictory conclusions are present in the literature [37].

ACKNOWLEDGMENTS

Colin Bousige and Adeline Lefevre are warmly thanked for their contribution in the synthesis and the analysis of samples at ambient conditions. We thank Jean-Louis Soubeyroux from Consortium de Recherches pour l'Emergence des Technologies Avancées (CRETA/CNRS, Grenoble, France) for the elaboration by arc-melting of the binary compounds used as reagents for the high-pressure synthesis.

[1] C. Cros, M. Pouchard, and P. Hagenmuller, C. R. Hebd. Seances Acad. Sci. **260**, 4764 (1965).
[2] J. S. Kasper, P. Hagenmuller, M. Pouchard, and C. Cros, Science **150**, 1713 (1965).
[3] C. Cros, M. Pouchard, P. Hagenmuller, and J. S. Kasper, Bull. Soc. Chim. Fr. **7**, 2737 (1965).
[4] J. Gallmeier, H. Schäfer, and A. Weiss, Z. Naturforsch. B **24b**, 665 (1969).
[5] A. San Miguel and P. Toulemonde, High Press. Res. **25**, 159 (2005).
[6] S. Bobev and S. C. Sevov, J. Solid State Chem. **92**, 153 (2000).
[7] G. S. Nolas, editor, *The Physics and Chemistry of Inorganic Clathrates, Vol. 199, Springer Series in Materials Science* (Springer, Heidelberg, 2015).
[8] A. San Miguel, P. Mélinon, D. Connétable, X. Blase, F. Tournus, E. Reny, S. Yamanaka, and J. P. Itié, Phys. Rev. B **65**, 054109 (2002).
[9] A. San Miguel, P. Kéghélian, X. Blase, P. Mélinon, A. Perez, J. P. Itié, A. Polian, E. Reny, C. Cros, and M. Pouchard, Phys. Rev. Lett. **83**, 5290 (1999).
[10] A. San Miguel, A. Merlen, P. Toulemonde, T. Kume, S. Le Floch, A. Aouizerat, S. Pascarelli, G. Aquilanti, O. Mathon, T. Le Bihan, J. P. Itié, and S. Yamanaka, Europhys. Lett. **69**, 556 (2005).
[11] L. Yang, Y. M. Ma, T. Iitaka, J. S. Tse, K. Stahl, Y. Ohishi, Y. Wang, R. W. Zhang, J. F. Liu, H.-K. Mao, and J. Z. Jiang, Phys. Rev. B **74**, 245209 (2006).
[12] J. S. Tse, R. Flacau, S. Desgreniers, T. Iitaka, and J. Z. Jiang, Phys. Rev. B **76**, 174109 (2007).
[13] J. S. Tse, L. Yang, S. J. Zhang, C. Q. Jin, Ch. J. Sahle, C. Sternemann, A. Nyrow, V. Giordano, J. Z. Jiang, S. Yamanaka, S. Desgreniers, and C. A. Tulk, Phys. Rev B **84**, 184105 (2011).
[14] T. Kume, H. Fukuoka, T. Koda, S. Sasaki, H. Shimizu, and S. Yamanaka, Phys Rev. Lett. **90**, 155503 (2003).
[15] J. S. Tse, S. Desgreniers, Z. Li, M. R. Ferguson, and Y. Kawazoe, Phys Rev. Lett. **89**, 195507 (2002).
[16] T. Kume, T. Koda, S. Sasaki, H. Shimizu, and J. S. Tse, Phys. Rev. B **70**, 052101 (2004).
[17] H. Shimizu, T. Kume, T. Kuroda, S. Sasaki, H. Fukuoka, and S. Yamanaka, Phys. Rev. B **68**, 212102 (2003).
[18] D. Machon, P. Toulemonde, P. F. McMillan, M. Amboage, A. Muñoz, P. Rodríguez-Hernández, and A. San Miguel, Phys. Rev. B **79**, 184101 (2009).

[19] A. C. Larson and R. B.V. Dreele, Los Alamos National Laboratory, Technical Report No. LAUR 86-748, 1994 (unpublished).
[20] H. Fukuoka, J. Kiyoto, and S. Yamanaka, J. Solid State Chem. **175**, 237 (2003).
[21] M. Hagelstein, A. San Miguel, A. Fontaine, and J. Goulon, J. Phys IV France **7**, C2-303 (1997).
[22] G. Aquilanti, W. A. Crichton, and S. Pascarelli, High Pres. Res. **23**, 301 (2003).
[23] J. Pellicer-Porres, A. San Miguel, and A. Fontaine, J. Synchrotron Radiation, **5**, 1250 (1998).
[24] A. P. Hammersley, S. O. Svensson, M. Hanfland, A. N. Fitch, and D. Hausermann, High Press. Res. **14**, 235 (1996).
[25] A. L. Ankudinov, B. Ravel, J. J. Rehr, and S. D. Conradson, Phys. Rev. B **58**, 7565 (1998).
[26] M. Newville, B. Ravel, D. H. Askel, J. J. Rehr, E. A. Stern, and Y. Yacbi, Physica B **154**, 208 (1995).
[27] M. L. Cohen, Phys. Rev. B, **32**, 7988 (1985).
[28] F. Schaffler, Semicond. Sci. Technol. **12**, 1515 (1997).
[29] P. Mélinon, X. Blase, A. San Miguel, and A. Perez, in *Nanosilicon* (Elsevier, Amsterdam, 2007), Chap. 2, pp. 79–113.
[30] *Properties of Silicon*. EMIS Datareviews Series No. 4 (INSPEC, 1988).
[31] P. Toulemonde, D. Machon, A. San Miguel, and M. Amboage, Phys. Rev. B **83**, 134110 (2011).
[32] F. Tournus, B. Masenelli, P. Mélinon, D. Connétable, X. Blase, A.-M. Flank, P. Lagarde, C. Cros, and M. Pouchard, Phys. Rev. B **69**, 035208 (2004).
[33] P. Tolédano and V. P. Dmitriev, *Reconstructive Phase Transitions* (Singapore, World Scientific, 1996).
[34] P. Bouvier and J. Kreisel, J. Phys.: Condens. Matter **14**, 3981 (2002).
[35] T. Iitaka, Phys. Rev. B **75**, 012106 (2007).
[36] H. Shimizu, T. Iitaka, T. Fukushima, T. Kume, S. Sasaki, N. Sata, Y. Ohishi, H. Fukuoka, and S. Yamanaka, J. Appl. Phys. **101**, 063549 (2007).
[37] T. Takabatake, K. Suekuni, T. Nakayama, and E. Kaneshita, Rev. Mod. Phys. **86**, 669 (2014).
[38] X. Zheng, S. Y. Rodriguez, and J. H. Ross, Jr., Phys. Rev. B **84**, 024303 (2011).
[39] D. Machon, F. Meersman, M. C. Wilding, M. Wilson, and P. F. McMillan, Prog Mat. Sci. **61**, 216 (2014).